



## OPEN ACCESS

## EDITED BY

Libo Tan,  
University of Alabama, United States

## REVIEWED BY

Jong-Sang Kim,  
Kyungpook National University,  
Republic of Korea  
Đura Nakarada,  
University of Belgrade, Serbia

## \*CORRESPONDENCE

Weili Liu  
✉ liuweili410@126.com  
Jiao Xu  
✉ xujiao@hljucm.edu.cn  
Wei Ma  
✉ mawei@hljucm.edu.cn

RECEIVED 17 December 2024

ACCEPTED 24 February 2025

PUBLISHED 12 March 2025

## CITATION

Kong L, Wu W, Li C, Ma L, Ma J, Pan M,  
Jiang S, Liu W, Xu J and Ma W (2025)  
Structure modification of luteolin and  
the influence of its derivatives on biological  
activities.  
*Front. Nutr.* 12:1546932.  
doi: 10.3389/fnut.2025.1546932

## COPYRIGHT

© 2025 Kong, Wu, Li, Ma, Ma, Pan, Jiang, Liu,  
Xu and Ma. This is an open-access article  
distributed under the terms of the [Creative  
Commons Attribution License \(CC BY\)](#). The  
use, distribution or reproduction in other  
forums is permitted, provided the original  
author(s) and the copyright owner(s) are  
credited and that the original publication in  
this journal is cited, in accordance with  
accepted academic practice. No use,  
distribution or reproduction is permitted  
which does not comply with these terms.

# Structure modification of luteolin and the influence of its derivatives on biological activities

Linyang Kong<sup>1</sup>, Wei Wu<sup>1</sup>, Chenliang Li<sup>1</sup>, Lengeng Ma<sup>1</sup>,  
Junbai Ma<sup>1</sup>, Meitong Pan<sup>1</sup>, Shan Jiang<sup>1</sup>, Weili Liu<sup>1\*</sup>, Jiao Xu<sup>1,2\*</sup>  
and Wei Ma<sup>1\*</sup>

<sup>1</sup>College of Pharmacy, Heilongjiang University of Chinese Medicine, Harbin, China, <sup>2</sup>College of Jiamusi, Heilongjiang University of Chinese Medicine (TCM), Jiamusi, China

**Introduction:** This research aims to synthesize luteolin derivatives from hemp seeds by means of chemical synthesis, improve the synthesis process, simplify the procedure, and increase the yield to obtain new luteolin derivatives. Additionally, anti-inflammatory and antioxidant activities of hemp seed extracts and newly synthesized substances are tested to screen out substances with high anti-inflammatory and antioxidant activities.

**Methods:** Using luteolin as the raw material, acetyl, propionyl, and butyryl groups are introduced into the molecular structure of luteolin. A one-pot synthesis method is employed to modify the hydroxyl groups at positions 5, 7, 3', and 4' to obtain six new luteolin acyl derivatives. The molar ratio of reaction conditions is 1:4. Pyridine (20 mL) is used as the solvent, and the reaction is carried out at 25°C and 110°C. Exploring the anti-inflammatory and antioxidant activities of luteolin and its derivatives by establishing a psoriasis model.

**Results:** The products are separated and purified by column chromatography and recrystallization, and six new luteolin acyl derivatives were synthesized: namely, 7,3',4'-tri-O-acetylated luteolin (A), 7,3',4'-tri-O-propionylated luteolin (B), 7,3',4'-tri-O-butyrylated luteolin (C), 5,7,3',4'-tetra-O-acetylated luteolin (D), 5,7,3',4'-tetra-O-propionylated luteolin (E), and 5,7,3',4'-tetra-O-butyrylated luteolin (F). By establishing a psoriasis like mouse model, the results showed that luteolin and its derivatives have good therapeutic effects on inflammation and antioxidation.

**Discussion:** Six new acyl derivatives of luteolin were synthesized through structural modification, which improved their solubility and bioavailability. In the psoriasis model, it has been proven that acyl derivatives of luteolin have anti-inflammatory and antioxidant activities, and have a relieving effect on psoriasis. Provide theoretical basis and potential treatment strategies for the future treatment of psoriasis.

## KEYWORDS

**hemp seeds, luteolin derivatives, structural modification, psoriasis, anti-inflammation, antioxidation**

## 1 Introduction

Hemp seeds are the dried and mature fruits of *Cannabis sativa* L. of the Moraceae family and are traditional crops with both medicinal and edible properties. Hemp seeds are sweet and neutral in nature, and enter the spleen, stomach, and large intestine meridians. They have the effect of moistening the intestines and promoting defecation and are used for blood deficiency and fluid depletion, and intestinal dryness and constipation. According to literature reports, hemp seeds contain various unsaturated fatty acids. In addition, there are also lignanamides

(1), cannabinoids (2), flavonoids, steroids and terpenes, alkaloids and other components. Modern pharmacological studies have shown that hemp seeds have effects such as antioxidation, anti-aging, anti-fatigue, anti-inflammation, neuroprotection, lipid regulation and liver protection, and immune regulation (3).

Luteolin is a typical natural flavonoid compound (4). It is widely distributed in nature and mainly exists in traditional Chinese medicinal materials such as honeysuckle, chrysanthemum, schizonepeta, herba ajugae, artichoke, callicarpa nudiflora, and hemp seeds. Luteolin also exists in various vegetables and fruits.

The C ring of luteolin is the key active component for antioxidation and scavenging free radicals, especially C'3-OH. The B-cyclic catechol structure of luteolin can contribute hydrogen electrons (H<sup>+</sup>), stabilize free radicals, thereby clearing harmful free radicals, protecting human cells or tissues, and delaying human aging. To further enhance the biological activity of luteolin, scholars have carried out various structural adjustments and modifications. In recent years, the research focus has mainly been on structural modifications such as alkylation, acylation, and salt formation on its phenolic hydroxyl groups (5).

Due to its excellent antioxidant (6), anti-inflammatory (7), and anticancer properties, luteolin has become the focus of natural drug research and application at home and abroad in recent years. In order to further improve the biological activity of luteolin, its structure has been modified. The most studied are substitution reactions such as alkylation and acylation at its active phenolic hydroxyl sites (8). The basic skeleton of luteolin is formed by two benzene rings A and B connected through a central three-carbon atom. The C7 on ring A and C'3 and C'4 on ring B all have active phenolic hydroxyl groups, but the phenolic hydroxyl group on C'3 is slightly less active than that on C7 and C'4. Wang Qiqin (9) used a one-pot method to remove active hydrogen, making this structure easy to undergo a nucleophilic reaction with RBr, and then obtain a mono-substituted compound of luteolin. Lü Pengcheng (10) first used 1,2-dibromoethane to form ring protection for C'3-OH and C'4-OH on its B ring, and then carried out various modification treatments on C7-OH on the A ring, such as alkylation and amination. Zhang Jiange (11) first protected C'3-OH and C'4-OH with dichlorodiphenylmethane, then introduced an alkane chain at the C7 position. Through the action of an aqueous solution of glacial acetic

acid or Pd (OH)<sub>2</sub>/C and H<sub>2</sub>, the protecting group was successfully removed and the selective retention of active hydroxyl groups was achieved. He Yaoyao (12) and others first carried out selective benzylation of luteolin with benzyl chloride, then carried out alkylation or acylation reactions, and finally obtained a series of 5-O-substituted derivatives by catalytic hydrogenolysis. Luteolin can undergo substitution reactions at different positions, as shown in Figure 1.

Using luteolin as the parent compound, structural modifications are carried out on the hydroxyl groups at positions 5, 7, 3', and 4' to obtain a series of new acylated derivatives, which improve its low solubility and bioavailability. The luteolin acylated derivatives obtained through chemical structure modification can broaden its biological activity and application range, providing new ideas for its research in anti-inflammatory, antioxidant, and other fields, providing experimental data for the development and application of new anti-inflammatory drugs, and also providing a theoretical basis for the derivatization of other flavonoid compounds.

Psoriasis, known as “Baibi” in traditional Chinese medicine, has typical symptoms including erythema accompanied by scales and itching (13). Psoriasis is a systemic inflammatory disease. Its pathogenesis is caused by the release of immune-related cells (such as macrophages, neutrophils, and T cells), the increase in pro-inflammatory cytokines (such as TNF- $\alpha$ , IL-17A, IL-23), and the chronic activation of the innate and adaptive immune systems, which leads to long-term damage to multiple tissues (such as skin tissue) and organs (such as the spleen) (14). It is mainly affected by two factors, namely genes and environment, including radiation, drugs, and microbial infections, etc., but there are differences in different regions (15).

Research has found that luteolin can inhibit various acute and chronic inflammations (16). Hall (17) also obtained similar findings when studying the structure–activity relationship of the anti-inflammatory activities of sesquiterpenes. When the exocyclic methylene group of Helenalin was saturated to form 2,3-Dihydrohelenalin, the inhibitory effect on rat paw swelling induced by carrageenan decreased from 75 to 38%.

Therefore, we took luteolin as the parent compound and introduced acetic anhydride, propionic anhydride, and butyric anhydride groups into the molecular structure of luteolin. We adopted the one-pot method

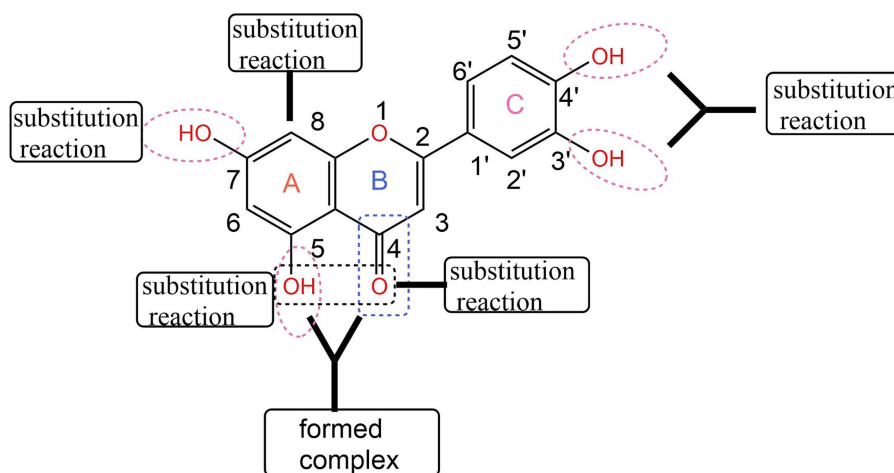


FIGURE 1  
Structural modification of luteolin (43).

for synthesis. Through the optimization of the synthesis process, the most suitable reaction conditions were screened out. Finally, the products were separated and purified by column chromatography and recrystallization methods. In this way, animal experiments were carried out to verify whether the six new luteolin derivatives still possess the anti-inflammatory and antioxidant activities of luteolin.

## 2 Experimental materials and methods

### 2.1 Grouping, modeling and administration methods

The animals used in the experiment were female BALB/c mice at the SPF level (7–8 weeks old, weighing 20–25 g). The experimental mice were raised in a pathogen-free animal room and had free access to food and water. The experimental mice were randomly divided into 17 groups, with 8 mice in each group. The backs of the mice were depilated using an electric shaver and depilatory cream, and relevant experiments were carried out 24 h later. In the experiment, on the backs of the mice in the model group (IMQ group), tacrolimus group (TK group), high-dose luteolin (Lut-H) group, high-dose luteolin derivative groups A-H, B-H, C-H, D-H, E-H, F-H, low-dose luteolin (Lut-L) group and low-dose luteolin derivative groups A-L, B-L, C-L, D-L, E-L, F-L, 62.5 mg of 5% imiquimod cream was applied every day. Four hours after the model was established, the positive drug tacrolimus (TK group) cream was evenly applied to the backs of the mice. The administration method of this positive drug was carried out concerning the existing literature and papers (12). For the administration groups, the luteolin solution at a dose of 80 mg/kg/d (Lut-H) and the luteolin derivative solutions at a dose of 80 mg/kg/d for the high-dose luteolin derivative groups were applied on the backs. For the low-dose luteolin (Lut-L) group and its low-dose luteolin derivative groups, the luteolin solution and derivative solutions at a dose of 40 mg/kg/d were, respectively, applied on the backs. Then, the blank group and the model group were smeared with petrolatum as a control. The mice were sacrificed on the 7th day of the experiment. Luteolin and its derivatives were formulated using polyethylene glycol 400. Skin samples from the backs of the mice were taken and thoroughly cleaned with a physiological saline solution. Part of them was fixed in 4% paraformaldehyde solution, and the other part was stored in a freezer at  $-80^{\circ}\text{C}$  to prepare for the subsequent experiments.

### 2.2 PASI score

After the application of the medication, the degree of psoriasis vulgaris symptoms on the back of the mice was scored by taking photos the next day (18). The PASI score is based on three indicators: scales, erythema, and infiltration, and is evaluated according to the severity of the symptoms. The degree of silver-like symptoms on the back skin of mice was ultimately determined based on the scoring results of scales, erythema, and infiltration (19).

### 2.3 H&E staining

Soak the back skin of mice in 4% paraformaldehyde, then dehydrate the tissue with different concentrations of alcohol for

transparency treatment. Subsequently, wax immersion treatment is carried out. The tissue was immersed in a mixture of xylene and paraffin, followed by three replacements with paraffin for 1 h each time. Put the skin tissue into the embedding machine for embedding. The embedded wax block is placed on a slicer for slicing, with a slice thickness of  $4\ \mu\text{m}$ . Before dewaxing, dry the slices in an oven for 30 min, then deparaffinize them with xylene and hydrate them in different concentrations of alcohol. After the above steps, the slices were placed in a staining solution (hematoxylin Harris) and stained for 5 min. After staining, the slices were sliced with xylene and finally sealed for observation (20).

### 2.4 Spleen index

The spleen is not only an important lymphoid organ but also the main place where T cells and B cells survive. Moreover, it is a crucial area for capturing antigens, recognizing antigens, and triggering immune responses. This organ can also indirectly reflect the degree of psoriasis-like symptoms. At the end of the last day of the experiment, the mice were treated with the cervical dislocation technique and were dissected thoroughly using biological dissection tools such as scissors, dissecting forceps and tweezers. During this process, we took out the spleens of the mice, photographed them and weighed to calculate the spleen index (21).

### 2.5 Enzyme-linked immunosorbent assay (ELISA) determination

Immunoassay technology relies on the highly selective and specific recognition and binding mechanism generated by specific antibodies with antigens or haptens, and is mainly used for accurate analysis and determination of the antibodies or antigens to be tested. Approximately 0.15 g of skin tissue from the backs of mice in each group stored in a  $-80^{\circ}\text{C}$  freezer was taken out. Firstly, the tissue on the backs of the mice needed to be cut into small pieces and then placed into 1.5 mL EP tubes. After that, 1.3 mL of cell lysis buffer was added and vortexed to mix evenly. Next, an ice bath was carried out for 30 min to fully lyse these cells. Finally, centrifuge for 15 min to collect the supernatant sample. ELISA kits containing IL-6 (serial number H007-1-2, antigen sequence number Uniprot NO: p08505) and TNF -  $\alpha$  (serial number H052-1-2, antigen sequence number Uniprot NO: p06804) were used to detect proteins in mouse back skin tissue samples (all kits were purchased from Jiancheng, Nanjing, China).

### 2.6 Determination of SOD enzyme activity and measurement of GSH and MDA contents in skin tissue

An appropriate amount of skin tissue from the backs of mice was taken from the  $-80^{\circ}\text{C}$  freezer and thawed on ice. A 100 mg portion of the tissue was then placed into a pre-cooled phosphate buffer solution and ground evenly using a tissue grinder. Then add 9 times the volume of normal saline for dilution to prepare a 10% skin tissue homogenate. Set the high-speed centrifuge to centrifuge at 3000 rpm for 10 min at  $4^{\circ}\text{C}$ . Collect the supernatant after each centrifugation

and repeat this process twice. The samples are then ready for the experiment. SOD (22), GSH (23), MDA (24) antioxidant assay kits were used to measure mouse skin tissue. The determination of various indicators was carried out according to the instructions of the kit [SOD (A001-3-2), GSH (A006-2-1) and MDA (A003-1-2) all kits were purchased from Jiancheng, Nanjing, China].

## 2.7 Data processing

Data were subjected to statistical analysis using the mean  $\pm$  standard deviation. The significant differences between data were analyzed using the Graphpad Prism (25) software. *p*-value of less than 0.05 was considered statistically significant.

## 3 Result

### 3.1 Impact on the degree of skin lesions in psoriasis mouse models

As shown in Figure 2, through the comparative analysis of the back skin conditions of mice in different groups, the healthy skin condition of the mice in the normal group can be clearly seen. The color of the backs of the mice gradually changed from the original light pink to a deeper and more extensive dark red, as if it were a sign of some kind of inflammatory reaction deep within the skin.

It is worth noting that on the 6th day after the use of the imiquimod drug, this change reached its peak. For the mice in the high-dose luteolin group and the high-dose luteolin derivative groups A, B, C, D, E, and F, the situation was slightly different. As shown in Figure 2D, there was smooth skin, a reduction in the thickening of the stratum corneum (Figure 2A), superficial erythema (Figure 2B), and a decrease in scales (Figure 2C). The low-dose luteolin group and the low-dose derivative groups A, B, C, D, E, and F did not seem to effectively alleviate the symptoms related to psoriasis. The severity of skin damage was evaluated based on the statistical data of the PASI score (Figures 2A–D). The scores of the normal group smeared with petrolatum were all 0. In the mice treated with imiquimod, the scores regarding psoriasis, cortex thickness and the degree of erythema all showed a gradually increasing pattern. As the number of days of drug administration increased, the PASI scores of the mice in the high-dose luteolin (80 mg/kg/d) group and the high-dose luteolin derivative groups A, B, C, D, E, and F in terms of erythema, scales and cortex thickness gradually decreased over time, which was similar to the performance of the mice in the tacrolimus group. Compared with the high-dose luteolin group, the high-dose luteolin derivative groups B, C, and D had similar effects and even surpassed the high-dose luteolin group.

### 3.2 Impact on the skin pathological changes of the psoriasis mouse model

Through histopathological analysis, the back skin samples of mice in each group were subjected to H&E staining (Figures 3A,B). In Figure 3, it was observed that the keratinocytes in the blank group

appeared in an orderly arrangement, indicating that they maintained a normal morphological and functional state in the tissue structure. This pathological feature reflects the balance and homeostasis of the mouse skin under the physiological environment. However, compared with the mice in the blank group, significant changes occurred on the backs of the mice with the psoriasis model induced by the application of imiquimod (26). The spinous cell layer of the epidermis not only thickened but was also accompanied by the downward extension of the epidermal layer and further thickening of the stratum corneum.

The results of H&E staining revealed that both high-dose luteolin and its derivatives exhibited significant anti-inflammatory effects. These compounds not only successfully inhibited the thickening of the stratum corneum and Munro's microabscess lesions caused by imiquimod but also effectively reduced the infiltration of inflammatory cells. Compared with the high-dose luteolin group, the high-dose groups of B-H and C-H performed even better in treating skin damage. However, when compared with the model group, the low-dose luteolin group and the luteolin derivative groups could also inhibit the epidermal thickening in mice induced by imiquimod. Although the phenomenon of Munro's microabscess occurred, which slightly damaged the structure of the epidermal layers, this thin barrier system still demonstrated its powerful resistance. In addition, this epidermal layer was also striving to reduce the keratinization process of the epidermis and tried its best to maintain the softness and smoothness of the skin surface. It indicates that the low-dose luteolin group and the luteolin derivative groups can also inhibit inflammatory cells.

### 3.3 Impact on the immune organs of the psoriasis mouse model

The results shown in Figure 4A indicate that, compared with the mice in the blank group, the volume of the spleens of the mice in the model group increased significantly. However, it is worth noting that although the spleen index of the model group was significantly higher than that of the blank group, when we delved deeper into the high-dose luteolin group and the high-dose luteolin derivative groups, we found that the spleens of these mice did not show the same volume increase phenomenon. On the contrary, their spleen indices (the ratio of spleen weight to body weight) were comparable to or even lower than that of the earlier blank group. The results revealed that the high-dose groups of C-H and D-H derivatives showed significant effects in alleviating the skin inflammation induced by imiquimod (Figure 4B).

### 3.4 Impact on skin inflammatory factors of the psoriasis mouse model

The enzyme-linked immunosorbent assay (ELISA) (27) was used to determine the changes in the contents of inflammatory factors in the skin lesions of psoriasis-like mice, to confirm that luteolin and its related derivatives have inhibitory effects on these inflammatory cytokines. The results shown in Figure 5A indicate that, compared with the control group, the expressions of the inflammatory cytokines TNF- $\alpha$  and IL-6 in the model group were significantly increased. However, the expressions of factors such as TNF- $\alpha$  and IL-6 in the positive drug group were significantly lower than those in the model

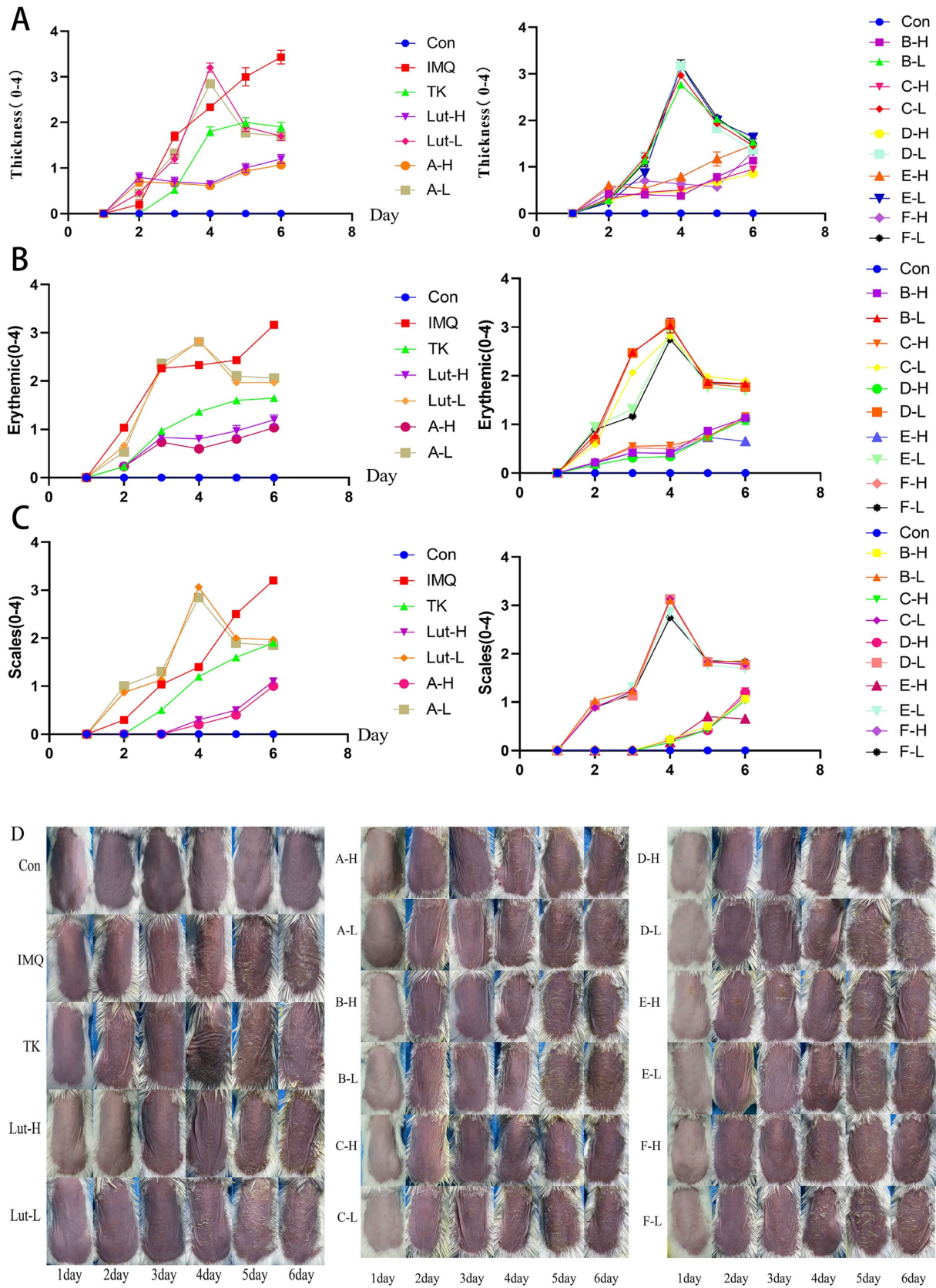
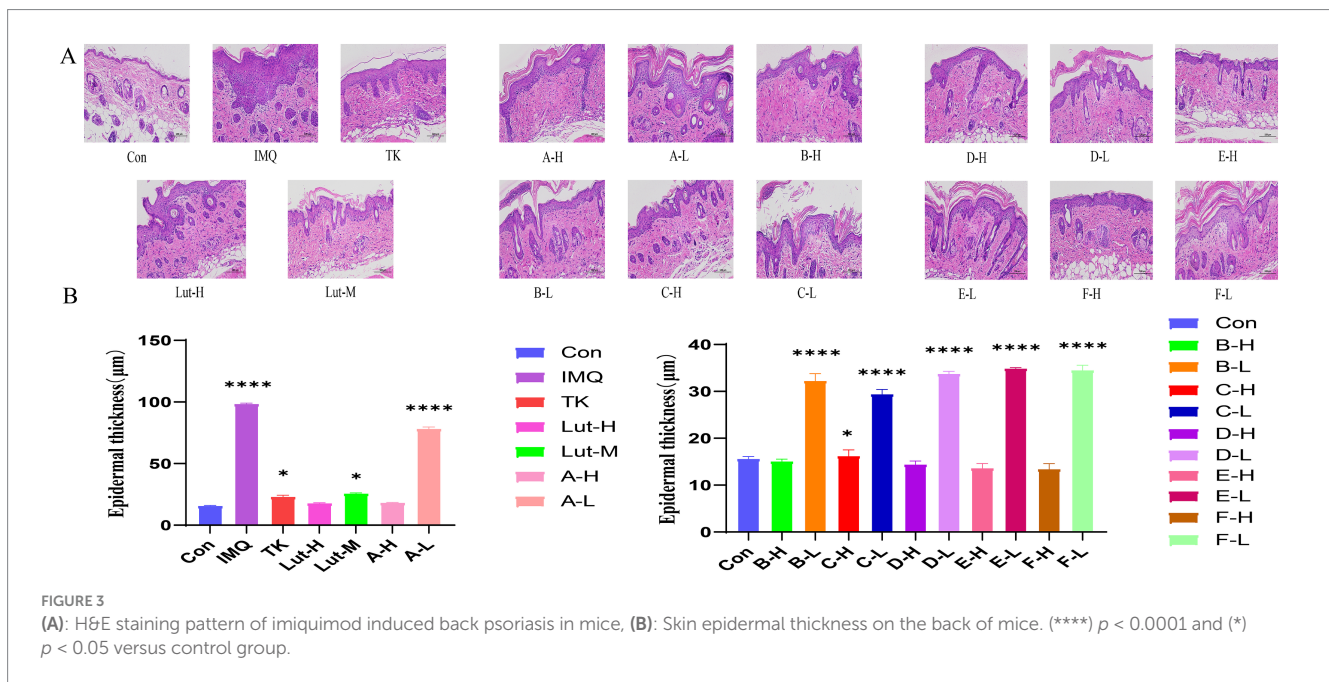


FIGURE 2 (A), (B) and (C): The PASI score for the back skin of mice, (D): Changes in the back skin of a mice psoriasis injury model induced by imiquimod.



group. The inhibitory effects of luteolin and its derivatives A-H, B-H, C-H, and F-H groups (80 mg/kg/d) on IL-6 were roughly the same as those of tacrolimus. In particular, the D-H and E-H groups had better effects in inhibiting inflammatory factors than the positive drug group. This reveals the potential therapeutic effects of luteolin and its derivatives on psoriasis, a common chronic skin disease (Figure 5B).

### 3.5 Impact on SOD activity, MDA and GSH contents in the supernatant of mouse skin tissue

The free-radical theory states that in the human body's antioxidant defense system, GSH and SOD antioxidant enzymes, as well as small-molecule non-enzymatic antioxidants and the generation of free radicals in the body are in a dynamic equilibrium (28). When this balance is disrupted, peroxides are produced in the body. Therefore, we measured the antioxidant indices. As observed in Figure 6A, when taking the blank group as a reference, the contents of SOD and GSH in the skin tissue of the mice in the model group decreased, while the content of MDA increased. Compared with the model group, the contents of SOD and GSH increased (Figures 6B,C), which led to a gradual improvement in the scavenging ability of GSH, and the content of lipid peroxidation products such as MDA decreased. The antioxidant activities of luteolin and its derivatives were better than those of the positive drug tacrolimus. In particular, the luteolin derivative groups A-H and E-H had better effects on increasing the content of SOD than the positive drug group. The luteolin derivative groups C-H and F-H had good effects on reducing the content of MDA, which were almost the same as those of the blank group mice. The luteolin derivative groups B-H and D-H had good effects on increasing the content of GSH, which were almost the same as the effects of the positive drug tacrolimus. Therefore, luteolin and its derivatives have a good antioxidant effect on the skin.

## 4 Experiment

### 4.1 Synthetic route of trisubstituted-O-acylation reaction

The structure of luteolin was modified with luteolin as the parent compound. The synthesis of trisubstituted derivatives A-C of luteolin with acetic anhydride, propionic anhydride and butyric anhydride is shown in the synthetic pathway in Figure 7.

### 4.2 Synthetic route of tetrasubstituted-O-acylation reaction

The synthesis of tetrasubstituted derivatives D-F of luteolin with acetic anhydride, propionic anhydride and butyric anhydride is shown in the synthetic pathway in Figure 8.

### 4.3 Structural characterization methods of luteolin derivatives

$^1\text{H}$  NMR spectra were recorded on Bruker 400 MHz spectrometer using DMSO- $d_6$  as solvent. Mass spectra were recorded on an ESI mass spectrometer. IR spectra were recorded with Bruker Tensor 27 series FT-IR spectrophotometer in KBr disks.

### 4.4 Target compound synthesis method

#### 4.4.1 7,3',4'-tri-O-acetylated luteolin (A)

Weigh 1 g (3.5 mmol) of luteolin and place it in a triangular flask. Add 20 mL of pyridine, stir with an electromagnetic stirrer, and react at 25°C. After the reaction solution becomes clear, add an appropriate amount of acetic anhydride to continue the reaction. Stir at room

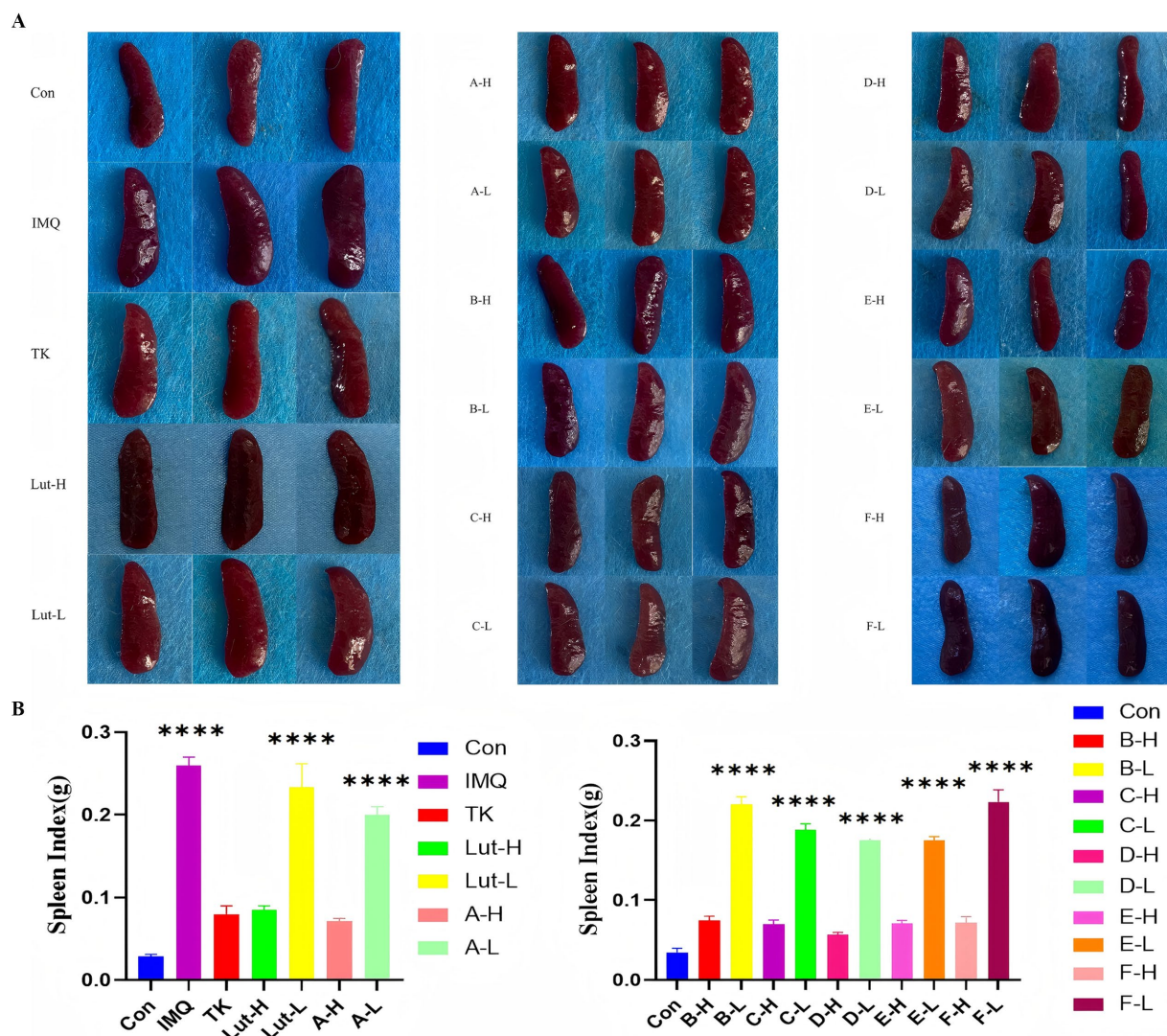


FIGURE 4 (A): Appearance map of spleens in each group of mice. (B): spleen index map of mice in each group. (\*\*\*\*)  $p < 0.0001$  versus control group.

temperature for 1 h, and detect the reaction by TLC. The developing agent is ethyl acetate: methanol = 1:1–4:1 (v/v). Filter the reaction mixture, separate the filtrate using a silica gel column, and elute with a gradient of ethyl acetate/methanol. Combine the eluents containing the product to recover the eluent, and recrystallize the residue from methanol to obtain a yellow solid product. The drying temperature is 180°C, the yield is 72%.  $m.p = 180^{\circ}\text{C}–180.1^{\circ}\text{C}$ ; IR(KBr)v: 3510, 3,078, 2,935, 1735, 1,489, 1,188,  $^1\text{H NMR}$ (400 MHz, DMSO- $d_6$ ) $\delta$ 12.90–12.66(m, 1H), 8.09–8.07 (m, 1H), 8.06–8.00 (m, 1H), 7.527.49 (m, 1H), 7.16 (s, 1H), 7.11 (t,  $J = 2.0$  Hz, 1H), 6.67(t,  $J = 2.0$  Hz, 1H), 2.34–2.30 (m, 9H,  $3 \times \text{CH}_3$ ).

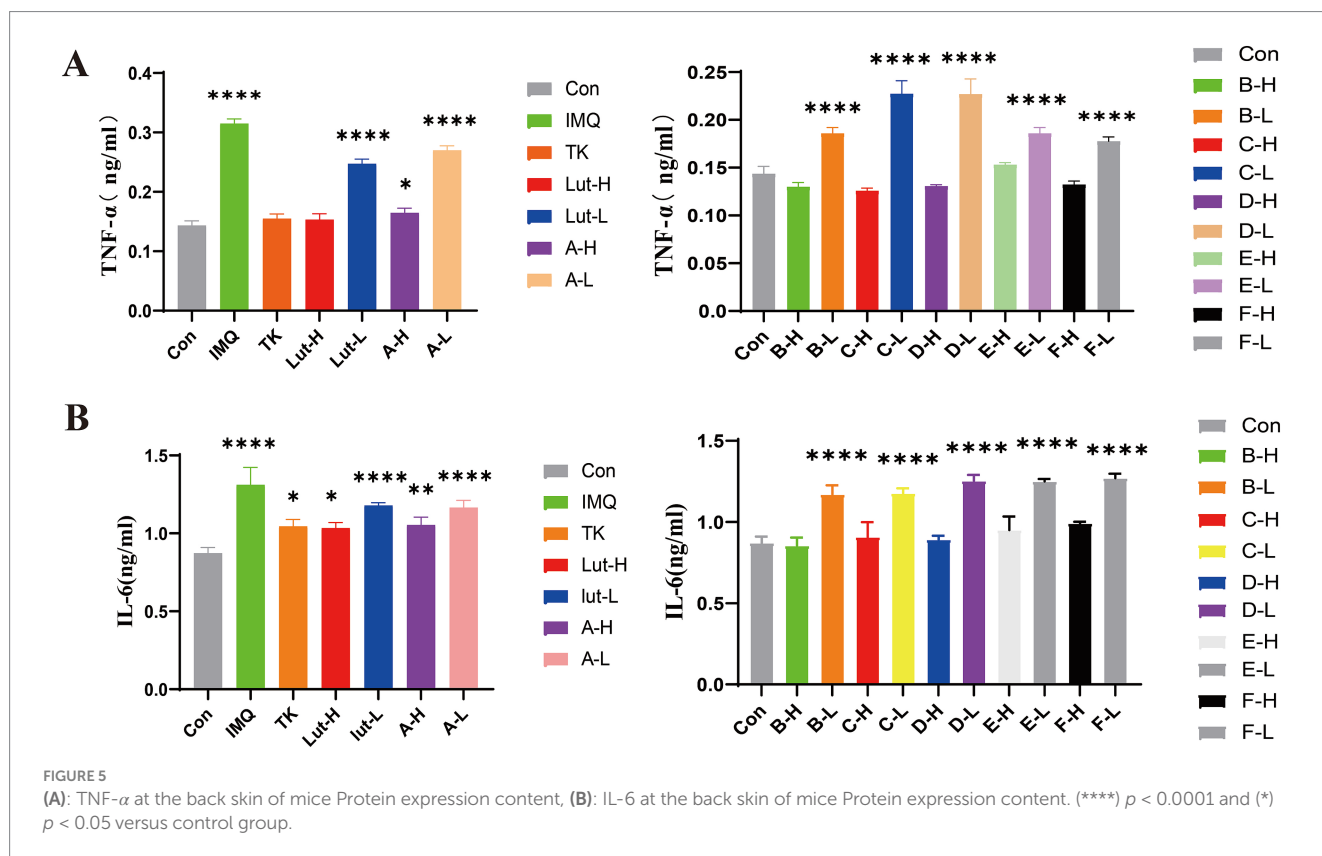
#### 4.4.2 7,3',4'-tri-O-propionylated luteolin (B)

Weigh 1 g (3.5 mmol) of luteolin and place it in a triangular flask. Add 20 mL of pyridine, stir with an electromagnetic stirrer, and react at 25°C. After the reaction solution becomes clear, add an appropriate amount of propionic anhydride to continue the reaction. Stir at room temperature for 1 h, and detect the reaction by TLC. The developing agent is ethyl acetate: methanol = 1:1–4:1

(v/v). Filter the reaction mixture, separate the filtrate using a silica gel column, and elute with a gradient of ethyl acetate/methanol. Combine the eluents containing the product to recover the eluent, and recrystallize the residue from methanol to obtain a yellow solid product. The drying temperature is 140°C, the yield is 76%.  $m.p = 144^{\circ}\text{C}–150^{\circ}\text{C}$ ; IR(KBr)v: 3387, 3,082, 2,980, 1785, 1,492, 1,188,  $^1\text{H NMR}$ (400 MHz, DMSO- $d_6$ )  $\delta$  12.90–12.66(m, 1H), 8.06–8.03 (m, 1H), 8.03–8.00(m, 1H), 7.50–7.49 (m, 1H), 7.16 (s, 1H), 7.10 (t,  $J = 2.0$  Hz, 1H), 6.65 (t,  $J = 2.0$  Hz, 1H), 2.26(m, 6H,  $3 \times \text{CH}_2$ ), 1.12 (m, 9H,  $3 \times \text{CH}_3$ ).

#### 4.4.3 7,3',4'-tri-O-butyrylated luteolin (C)

Weigh 1 g (3.5 mmol) of luteolin and place it in a triangular flask. Add 20 mL of pyridine, stir with an electromagnetic stirrer, and react at 25°C. After the reaction solution becomes clear, add an appropriate amount of succinic anhydride to continue the reaction. Stir at room temperature for 1 h, and detect the reaction by TLC. The developing agent is ethyl acetate: methanol = 1:1–4:1 (v/v). Filter the reaction mixture, separate the filtrate using a silica



gel column, and elute with a gradient of ethyl acetate/methanol. Combine the eluents containing the product to recover the eluent, and recrystallize the residue from methanol to obtain a yellow solid product. The drying temperature is 150°C, the yield is 75%.  $m.p = 157^{\circ}\text{C}-162^{\circ}\text{C}$ ; IR(KBr)v: 3510, 3,082, 2,966, 1782, 1,492, 1,125,  $^1\text{H NMR}$ (400 MHz, DMSO- $d_6$ ) $\delta$  12.83–12.61(m,1H), 8.13–7.92(m, 2H), 7.52–7.43(m, 1H), 7.18(s, 1H), 7.11 (t,  $J = 1.9$  Hz, 1H), 6.65 (t,  $J = 1.9$  Hz, 1H), 2.67–2.55 (m, 6H, 3  $\times$  CH<sub>2</sub>), 1.70–1.50 (m, 6H, 3  $\times$  CH<sub>2</sub>), 1.08–0.85 (m, 9H, 3  $\times$  CH<sub>3</sub>).

#### 4.4.4 5,7,3',4'-tetra-O-acetylated luteolin (D)

Weigh 1 g (3.5 mmol) of luteolin and place it in a triangular flask. Add 20 mL of pyridine and stir with an electromagnetic stirrer for 10 min. Allow the reaction to proceed at room temperature. Once the reaction solution is clear, add an appropriate amount of acetic anhydride and continue the reaction at 110°C until the reaction stops. The reaction was detected by TLC, and the developing agent was ethyl acetate:methanol = 1:1–4:1 (v/v). Filter the reaction mixture, separate the filtrate using a silica gel column, and elute with a gradient of ethyl acetate/methanol. Combine the eluents containing the product to recover the eluent, and recrystallize the residue from methanol to obtain a yellow solid product. The drying temperature is 220°C, the yield is 78%.  $m.p = 226^{\circ}\text{C}-227^{\circ}\text{C}$ ; IR(KBr)v: 3510, 3,070, 2,939, 1774,1,508,1,188,  $^1\text{H NMR}$  (400 MHz, DMSO- $d_6$ )  $\delta$  8.06–7.96 (m, 2H), 7.61 (d,  $J = 4.5$  Hz,1H), 7.48 (dd,  $J = 8.0, 4.0$  Hz, 1H), 7.12–7.03 (m, 1H), 6.93 (s,1H), 2.35–2.30 (m,12H,4  $\times$  CH<sub>3</sub>).

#### 4.4.5 5,7,3',4'-tetra-O-propionylated Luteolin (E)

Weigh 1 g (3.5 mmol) of luteolin and place it in a triangular flask. Add 20 mL of pyridine and stir with an electromagnetic stirrer for 10 min. Allow the reaction to proceed at room temperature. Once the reaction solution is clear, add an appropriate amount of succinic anhydride and continue the reaction at 110°C until the reaction stops. The reaction was detected by TLC, and the developing agent was ethyl acetate:methanol = 1:1–4:1 (v/v). Filter the reaction mixture, separate the filtrate using a silica gel column, and elute with a gradient of ethyl acetate/methanol. Combine the eluents containing the product to recover the eluent, and recrystallize the residue from methanol to obtain a yellow solid product. The drying temperature is 160°C, the yield is 82%.  $m.p = 165^{\circ}\text{C}-166^{\circ}\text{C}$ ; IR(KBr)v: 3522, 3,082, 2,985, 1785, 1,504, 1,125,  $^1\text{H NMR}$  (400 MHz, DMSO- $d_6$ )  $\delta$  8.10–7.97 (m, 2H), 7.63 (t,  $J = 1.9$  Hz,1H), 7.54–7.40 (m, 1H), 7.07 (t,  $J = 1.9$  Hz,1H), 6.94 (s, 1H), 2.72–2.57 (m, 8H, 4  $\times$  CH<sub>2</sub>), 1.21–1.02 (m, 12H, 4  $\times$  CH<sub>3</sub>).

#### 4.4.6 5,7,3',4'-tetra-O-butyrylated luteolin (F)

Weigh 1 g (3.5 mmol) of luteolin and place it in a triangular flask. Add 20 mL of pyridine and stir with an electromagnetic stirrer for 10 min. Allow the reaction to proceed at room temperature. Once the reaction solution is clear, add an appropriate amount of succinic anhydride and continue the reaction at 110°C until the reaction stops. The reaction was detected by TLC, and the developing agent was ethyl acetate:methanol = 1:1–4:1 (v/v). Filter the reaction mixture, separate

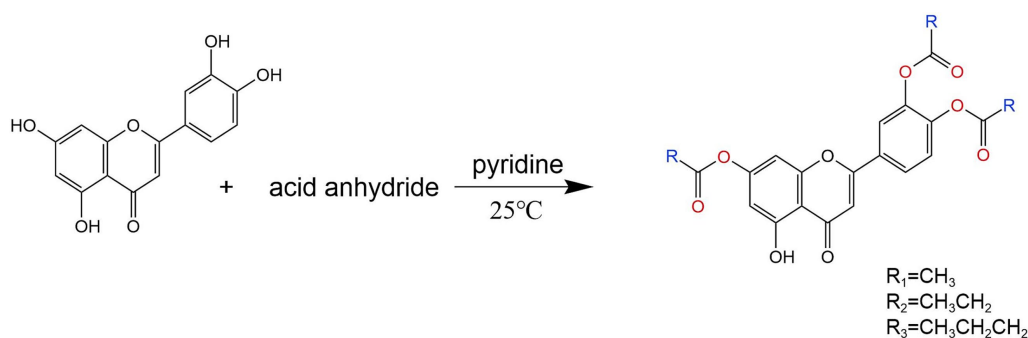
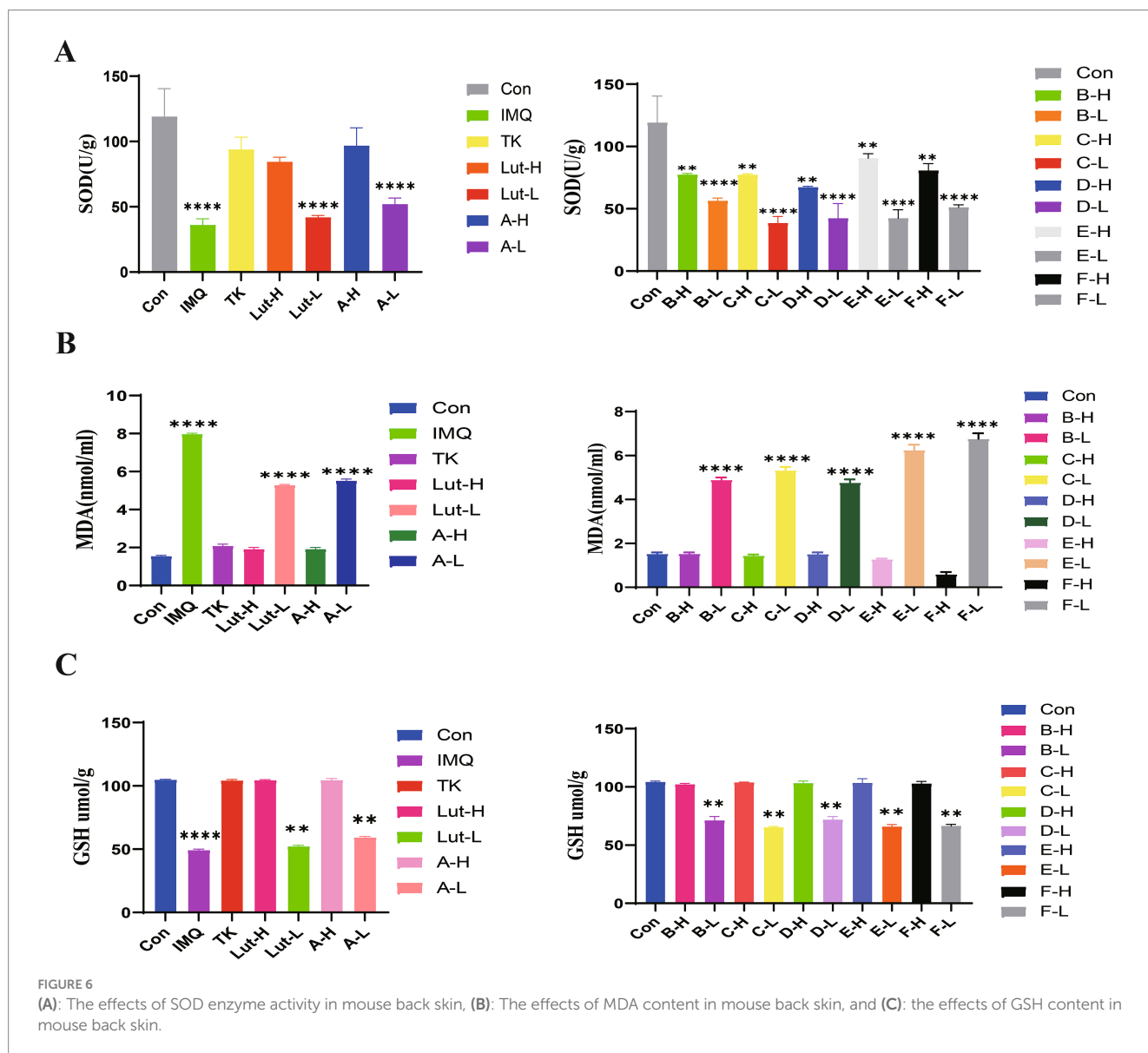
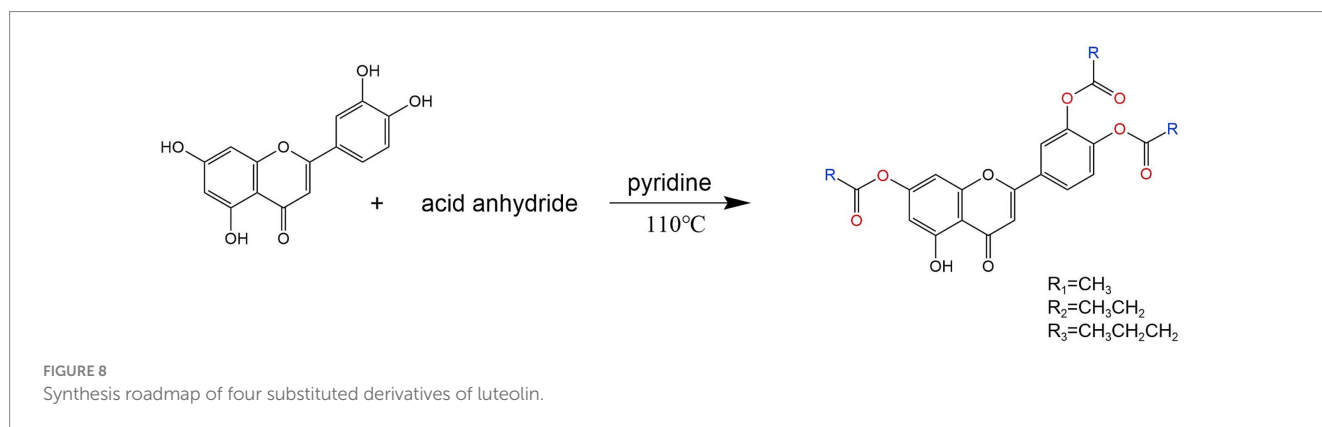


**FIGURE 7**  
 Synthesis roadmap of three substituted derivatives of luteolin.

the filtrate using a silica gel column, and elute with a gradient of ethyl acetate/methanol. Combine the eluents containing the product to recover the eluent, and recrystallize the residue from methanol to obtain a yellow solid product. The drying temperature is 150°C, the yield is 83%.

$m.p = 150^\circ\text{C}-151^\circ\text{C}$ ; IR(KBr)v: 3487, 3090, 2970, 1779, 1508, 1188,  $^1\text{H}$  NMR (400 MHz, DMSO- $d_6$ )  $\delta$  8.06–7.95 (m, 2H), 7.62 (d,  $J = 1.8$  Hz, 1H), 7.55–7.39 (m, 1H), 7.05 (t,  $J = 1.8$  Hz, 1H), 6.95 (s, 1H), 2.68–2.55 (m, 8H, 4  $\times$  CH $_2$ ), 1.79–1.56 (m, 8H, 4  $\times$  CH $_2$ ), 1.03–0.87



(m,12H,4 × CH<sub>3</sub>). The above spectra are all shown in Supplementary Figure 1.

## 5 Discussion

To obtain new luteolin derivatives, this study mainly took luteolin as the parent compound and used acetic anhydride, propionic anhydride and butyric anhydride as raw materials for synthesis by the one-pot method. This synthesis procedure is simple, the reaction is controllable, the products are easy to separate, and there are few by-products. Through the optimization of reaction conditions, the yield of the acylated products of luteolin has been improved. Moreover, the solubility of these products in aqueous solutions and alcohol solutions was investigated. The solubility of the acylated products A, B, C, D, E, and F in hot water is slightly better than that of luteolin, with product A having the best solubility. Compared with the solubility in aqueous solutions, the acylated products A, B, C, and D have better solubility in polyethylene glycol solutions. And their structures were characterized by means of infrared spectroscopy, hydrogen nuclear magnetic resonance spectroscopy and other technical means. The results showed that the synthesis of this kind of compound laid a good foundation for further chemical modifications on the 5th, 7th, 3', and 4' positions of luteolin compounds.

In our study, luteolin and a series of luteolin derivatives have a significant inhibitory effect on imiquimod-induced psoriasis in mice. Though the Psoriasis Area and Severity Index (PASI) score, spleen index and hematoxylin and eosin (H&E) staining, it was demonstrated that the acylated derivatives of luteolin can improve skin damage, reduce the infiltration of inflammatory factors, and have a significant anti-inflammatory effect. The acylated derivatives of luteolin inhibit imiquimod-induced psoriasis lesions in mice by down-regulating the expressions of TNF- $\alpha$  and IL-6 in the mouse skin tissue, increasing the contents of superoxide dismutase (SOD) and glutathione (GSH), and reducing the content of malondialdehyde (MDA). Among them, the high-dose groups of luteolin derivatives such as A-H, E-H and F-H exert the same antioxidant effect as tacrolimus, and even the groups of derivatives B-H, C-H and D-H are superior to the effects of the positive drug tacrolimus and the high-dose group of luteolin. They can not only significantly alleviate the skin symptoms of mice with psoriasis but also show a good repairing effect on various tissue damages caused by psoriasis. This finding provides brand-new ideas and directions for the research and development of drugs related to psoriasis.

There are many synthetic methods for luteolin derivatives, mainly including modifications of hydroxyl groups, carbonyl

groups, and modifications of A and B rings. Through the optimization of synthetic methods, luteolin derivatives with good solubility and high bioavailability can be obtained. Lo (29) designed nine acyl derivatives with different structures and obtained tri-O-benzyl luteolin through chemical reactions between themselves and benzyl bromide. On this basis, by adding acyl chloride - triethylamine as raw materials, derivatives of 5-O-acyl tri-O-benzyl luteolin were synthesized. Fischer (30) reacted luteolin with an excess of fatty acid acyl chlorides and obtained tetra-acylated luteolin derivatives. Zhou Meirong (31) carried out the Mannich reaction between the H bond at the C-8 position of ring A of luteolin and primary aliphatic amines in an aqueous solution of acetaldehyde and discovered ten new 8-aminomethylated derivatives.

In this study, the one-pot method was used to conduct structural modifications on the hydroxyl groups at the 5th, 7th, 3' and 4' positions of luteolin, and a total of six new acylated derivatives of luteolin were synthesized. This synthesis method is simple to operate and has a high yield. In the experiment, the influences of reaction temperature and reaction time on the synthesis were investigated. It was found that if the reaction temperature was too low, the reaction could not proceed. On the other hand, if the temperature was too high, the by-products of the reaction would increase, resulting in a low yield. Moreover, different luteolin derivatives were synthesized at different temperatures. The acylated products A, B, and C were synthesized at 25°C, while the acylated products D, E, and F were synthesized at 110°C. The reaction time had little impact on this experiment. Based on conditions such as the clarity of the solution during the reaction, the yield of derivatives, and the reduction of substitution by-products, 90 min was selected as the optimal reaction time. To compare the one-pot method with the synthesis methods recorded in the literature, there was no difference in yield. However, the method in literature (32) was complicated, required strict control of conditions, and was difficult in separate. In contrast, the one-pot method was relatively simple in design, easy to control the conditions, and easy to separate. The water solubility and lipid solubility of luteolin were poor. Luteolin was almost insoluble in cold water and slightly soluble in hot water. Osonga (33) reacted luteolin with dibenzyl diphosphate and synthesized luteolin tetraphosphate. The solubility of this compound in water is 297 times that of luteolin. Tsai (34) solved the problem of the difficulty in dissolving luteolin in water and synthesized three water-soluble luteolin phosphate substances, laying a foundation for the development of its derivatives. Among the six luteolin derivatives generated in this chapter, after testing, it was found that the water solubilities of derivatives A and B were better than that of luteolin, and the solubilities of derivatives A, B, C, D, E and F in alcohol solutions were all better than that of luteolin, indicating that the introduction of acetic

anhydride and propionic anhydride groups increased the solubility of luteolin.

Currently, in the treatment of psoriasis, the chemical components found in traditional Chinese medicine have been isolated and used as independent extracts or monomers. In this chapter, we applied imiquimod on the backs of mice to create a psoriasis-like model, aiming to study the inhibitory effect of luteolin and its derivatives on psoriasis-like symptoms. From different perspectives, we preliminarily explored the role of luteolin and luteolin derivatives in inhibiting psoriasis-like symptoms using ELISA experiments and other methods.

Previous studies have found that luteolin can significantly inhibit cell growth, remarkably reduce skin oxidative stress, and exhibit excellent antioxidant properties (35, 36). Based on the results analysis of the Psoriasis Area and Severity Index (PASI) score, spleen measurement and hematoxylin and eosin (H&E) staining methods in this study, it was discovered that both high-dose and low-dose luteolin and luteolin derivatives can alleviate scales, erythema and the thickness of the cortex, relieve the symptoms of splenomegaly, and reduce the occurrence of microabscess lesions in the model group. This implies that luteolin and luteolin derivatives A, B, C, D, E, and F have a certain inhibitory effect on psoriasis-like symptoms. This is consistent with previous studies (37). Based on the above research findings, luteolin has shown a repairing effect on the skin damage caused by psoriasis, which means that it has the potential to become a topical drug for the treatment of psoriasis.

Studies have shown that luteolin exhibits excellent anti-inflammatory effects and can inhibit the release of various inflammatory factors, thereby alleviating the inflammatory response of tissues (38, 39). In the psoriasis animal model, there are a large number of inflammatory cells, such as IL-6, TNF- $\alpha$ , etc. The ELISA method was used to detect the expression of inflammatory factors in the skin lesion tissues of mice. In addition, the oxidative stress response accelerates the inflammatory response through a variety of signal pathways, including NF- $\kappa$ B and mitogen-activated protein kinases. Studies have found that antioxidants can regulate psoriasis symptoms, further indicating that oxidative stress plays an important role in psoriasis (40). It protects cell membranes from damage by scavenging hydroxyl radicals, hydrogen peroxide, and peroxides. MDA is used as an indicator to evaluate the level of lipid peroxidation. In various pathological and skin damage model groups of psoriasis, its level exceeds that of the blank group. Therefore, MDA is regarded as a key indicator for evaluating the condition of psoriasis and the curative effect of drug treatment (41). GSH has the function of scavenging free radicals and can slow down the lipid peroxidation reaction (42). This study found that luteolin and luteolin derivatives can down-regulate the expressions of inflammatory factors such as IL-6 and TNF- $\alpha$ , can also increase the activity of SOD enzyme and the content of GSH in the skin tissue induced by imiquimod, and at the same time can reduce the content of MDA, further inhibit the release of free radicals, thereby enhancing the body's anti-inflammatory and antioxidant abilities and having the effect of treating psoriasis.

## 6 Conclusion

The structure of luteolin has been carefully adjusted and modified, and six acyl derivatives of luteolin have been successfully synthesized. By analyzing the influences of reaction time, reaction

temperature, and the molar amounts of luteolin, acetic anhydride, propionic anhydride, and butyric anhydride on the synthesis of acyl derivatives, the optimal synthesis conditions were finally determined. Moreover, through the structural analysis of the acyl derivatives of luteolin, it can be known that such derivatives have formed stable structures and possess good solubility. Therefore, it has also been confirmed in the psoriasis model that the acyl derivatives of luteolin possess anti-inflammatory and antioxidant activities and exhibit the effect of alleviating psoriasis. It has been found that compounds A-H, E-H, and F-H have a good effect on alleviating psoriasis, which is equivalent to the efficacy of luteolin and tacrolimus, while the activities of B-H, C-H, and D-H are higher than that of the positive drug tacrolimus. The results of spectral analysis (IR,  $^1\text{H}$  NMR) have verified all the synthesized compounds.

## Data availability statement

The datasets presented in this study can be found in online repositories. The names of the repository/repositories and accession number(s) can be found in the article/[Supplementary material](#).

## Ethics statement

The animal study was approved by the Ethics Committee of Heilongjiang University of Chinese Medicine. The study was conducted in accordance with the local legislation and institutional requirements. The study was conducted in accordance with the local legislation and institutional requirements.

## Author contributions

LK: Conceptualization, Writing – original draft. WW:–. CL: Data curation, Writing – review & editing. LM: Investigation, Resources, Writing – review & editing. JM: Investigation, Resources, Writing – review & editing. MP: Investigation, Resources, Writing – review & editing. SJ: Investigation, Resources, Writing – review & editing. WL: Funding acquisition, Supervision, Writing – review & editing. JX: Supervision, Writing – review & editing. WM: Funding acquisition, Supervision, Writing – review & editing.

## Funding

The author(s) declare that financial support was received for the research, authorship, and/or publication of this article. Project name: Study on the Chemical Components of Chinese Herbal Medicine Hemp Seed and Analysis of the Biological Activity of Cannabidiol (2023yjscx025), Sponsor: LK; National Key Research and development Project, research and demonstration of collection, screening and breeding technology of ginseng and other genuine medicinal materials, Project No.2021YFD1600901, Sponsor: WM; Heilongjiang Province “double first-class” discipline collaborative innovation achievement project: Quality optimization and deep processing of

characteristic Chinese medicinal materials in the lower cold region of great health industry, Project No. LJGXCG2023-058, Sponsor: WM.

## Conflict of interest

The authors declare that the research was conducted in the absence of any commercial or financial relationships that could be construed as a potential conflict of interest.

## Generative AI statement

The authors declare that no Gen AI was used in the creation of this manuscript.

## References

- Ren Y, Xu Z, Qiao Z, Wang X, Yang C. Flaxseed Lignan alleviates the paracetamol-induced hepatotoxicity associated with regulation of gut microbiota and serum metabolome. *Nutrients*. (2024) 16:295. doi: 10.3390/nu16020295
- Yoo EH, Lee JH. Cannabinoids and their receptors in skin diseases. *Int J Mol Sci*. (2023) 24:16523. doi: 10.3390/ijms242216523
- Occhiuto C, Aliberto G, Ingegneri M, Trombetta D, Circosta C, Smeriglio A. Comparative evaluation of the nutrients, phytochemicals, and antioxidant activity of two hempseed oils and their byproducts after cold pressing. *Molecules*. (2022) 27:3431. doi: 10.3390/molecules27113431
- Ming-Xin Guo MM, Wu X, Feng YF, Hu ZQ. Research Progress on the structural modification of Magnolol and Honokiol and the biological activities of their derivatives. *Chem Biodivers*. (2023) 20:e202300754. doi: 10.1002/cbdv.202300754
- ID K, Nur ÖF, Mustafa Ç, Sadik OA. Synthesis, biological and computational studies of flavonoid acetamide derivatives. *RSC Advances*. (2022) 12:10037–50. doi: 10.1039/D2RA01375D
- Wang Y, Liu X-J, Chen J-B, Cao J-P, Li X, Sun C-D. Citrus flavonoids and their antioxidant evaluation. *Crit Rev Food Sci Nutr*. (2021) 62:3833–54. doi: 10.1080/10408398.2020.1870035
- Jang J-H, Lee T-J. Mechanisms of phytochemicals in anti-inflammatory and anti-cancer. *Int J Mol Sci*. (2023) 24:7863. doi: 10.3390/ijms24097863
- Ozawa HMT, Burdeos GC, Miyazawa T. Biological functions of antioxidant dipeptides. *J Nutr Sci Vitaminol (Tokyo)*. (2022) 68:162–71. doi: 10.3177/jnsv.68.162
- Gam JJ, DiAndreth B, Jones RD, Huh J, Weiss R. A 'poly-transfection' method for rapid, one-pot characterization and optimization of genetic systems. *Nucleic Acids Res*. (2019) 47:e106. doi: 10.1093/nar/gkz623
- Peng-Cheng L, Huan-Qiu L, Xue JY, Shi L, Zhu HL. Synthesis and biological evaluation of novel luteolin derivatives as antibacterial agents. *Eur J Med Chem*. (2009) 44:908–14. doi: 10.1016/j.ejmech.2008.01.013
- Zhang J, Liu X, Lei X, Wang L, Guo L, Zhao G, et al. Discovery and synthesis of novel luteolin derivatives as DAT agonists. *Bioorg Med Chem*. (2010) 18:7842–8. doi: 10.1016/j.bmc.2010.09.049
- Jiang Z-B, Wang W-J, Xu C, Xie Y-J, Wang X-R, Zhang Y-Z, et al. Luteolin and its derivative apigenin suppress the inducible PD-L1 expression to improve anti-tumor immunity in KRAS-mutant lung cancer. *Cancer Lett*. (2021) 515:36–48. doi: 10.1016/j.canlet.2021.05.019
- Orsmond A, Bereza-Malcolm L, Lynch T, March L, Xue M. Skin barrier dysregulation in psoriasis. *Int J Mol Sci*. (2021) 22:10841. doi: 10.3390/ijms221910841
- Griffiths CEM, Armstrong AW, Gudjonsson JE, Barker JNWN. Psoriasis. *Lancet*. (2021) 397:1301–15. doi: 10.1016/S0140-6736(20)32549-6
- Rendon A, Schäkel K. Psoriasis pathogenesis and treatment. *Int J Mol Sci*. (2019) 20:1475. doi: 10.3390/ijms20061475
- Gendrisch F, Esser PR, Schempp CM, Wölfl U. Luteolin as a modulator of skin aging and inflammation. *Biofactors*. (2020) 47:170–80. doi: 10.1002/biof.1699
- Hall IHLK, Mar EC, Starnes CO, Waddell TG. Antitumor agents. 21. A proposed mechanism for inhibition of cancer growth by tenulin and helenalin and related cyclopentenones [J]. *J Med Chem*. (1977) 20:333–7. doi: 10.1021/jm00213a003
- Gao J, Chen F, Fang H, Mi J, Qi Q, Yang M. Daphnetin inhibits proliferation and inflammatory response in human HaCaT keratinocytes and ameliorates imiquimod-induced psoriasis-like skin lesion in mice. *Biol Res*. (2020) 53:48. doi: 10.1186/s40659-020-00316-0
- Otero ME, van Geel MJ, Hendriks JCM, van de Kerkhof PCM, Seyger MMB, de Jong EMGJ. A pilot study on the psoriasis area and severity index (PASI) for small areas:

## Publisher's note

All claims expressed in this article are solely those of the authors and do not necessarily represent those of their affiliated organizations, or those of the publisher, the editors and the reviewers. Any product that may be evaluated in this article, or claim that may be made by its manufacturer, is not guaranteed or endorsed by the publisher.

## Supplementary material

The Supplementary material for this article can be found online at: <https://www.frontiersin.org/articles/10.3389/fnut.2025.1546932/full#supplementary-material>

- presentation and implications of the low PASI score. *J Dermatol Treat*. (2014) 26:314–7. doi: 10.3109/09546634.2014.972316
- Wang C, Yue F, Kuang S. Muscle histology characterization using H&E staining and muscle Fiber type classification using immunofluorescence staining. *Bio-Protoc*. (2017) 7:e2279. doi: 10.21769/BioProtoc.2279
- Carrillo D, Edwards N, Arancibia-Altamirano D, Otárola F, Villarroel C, Prieto CP, et al. Efficacy of stem cell secretome loaded in hyaluronate sponge for topical treatment of psoriasis. *Bioeng Transl Med*. (2023) 8:e10443. doi: 10.1002/btm2.10443
- Liu C, Sun W, Li N, Gao J, Yu C, Wang C, et al. Schisantherin A improves learning and memory of mice with D-galactose-induced learning and memory impairment through its Antioxidation and regulation of p19/p53/p21/cyclin D1/CDK4/RBGene expressions. *J Med Food*. (2018) 21:678–88. doi: 10.1089/jmf.2017.4090
- Rahman I, Kode A, Biswas SK. Assay for quantitative determination of glutathione and glutathione disulfide levels using enzymatic recycling method. *Nat Protoc*. (2007) 1:3159–65. doi: 10.1038/nprot.2006.378
- Gerard Drewa EK-M, Woźniak A, Protas-Drozd F, Mila-Kierzenkowska C, Rozwodowska M, Kowalyszyn B, Rafał Czajkowski activity of superoxide dismutase and catalase and the level of lipid peroxidation products reactive with TBA in patients with psoriasis. *Med Sci Monit*. (2002) 8:BR338.
- Mitteer DR, Greer BD. Publisher correction to: using GraphPad Prism's heat maps for Efcient, fine-grained analyses of single-case data. *Behav Anal Pract*. (2022) 15:515. doi: 10.1007/s40617-022-00678-9
- Balan R, Grigoras A, Popovici D, Amalinei C. The histopathological landscape of the major psoriasisiform dermatoses. *Arch Clin Cases*. (2019) 6:59–68. doi: 10.22551/2019.24.0603.10155
- Hornbeck PV. Enzyme-linked immunosorbent assays. *Curr Protoc Immunol*. (2015) 110:2.1.1–2.1.23. doi: 10.1002/0471142735.im0201s110
- He L, He T, Farrar S, Ji L, Liu T, Ma X. Antioxidants maintain cellular redox homeostasis by elimination of reactive oxygen species. *Cell Physiol Biochem*. (2017) 44:532–53. doi: 10.1159/000485089
- Stephen Lo, Euphemia Leung, Bruno Fedrizzi, David Barker, et al. Syntheses of mono-acylated luteolin derivatives, evaluation of their antiproliferative and radical scavenging activities and implications on their oral bioavailability. *Sci Rep* (2021);11, doi: 10.1038/s41598-021-92135-w:12595, PMID: PMC8206097.
- Fabian F, Evelynne Z, Jean-Marc B, Julien H, Fabrice M. UV-ABC screens of luteolin derivatives compared to edelweiss extract. *J Photochem Photobiol B Biol*. (2011) 103:8–15. doi: 10.1016/j.jphotobiol.2011.01.005
- Da Re P, Verlicchi L, Setnikar I, Murmann W, Magistretti MJ. N-substituted 7-methoxy-8-aminomethyl-chromones and flavones: new brain-stem stimulants. *Nature*. (1959) 1:362–3.
- Defant A, Mancini I. Design, synthesis and Cancer cell growth inhibition evaluation of new Aminoquinone hybrid molecules. *Molecules*. (2019) 24:2224. doi: 10.3390/molecules24122224
- Osonga FJ, Le P, Luther D, Sakhaee L, Sadik OA. Water-based synthesis of gold and silver nanoparticles with cuboidal and spherical shapes using luteolin tetraphosphate at room temperature. *Environ Sci Nano*. (2018) 5:917–32. doi: 10.1039/C8EN00042E
- Tsai H-Y, Chen M-Y, Hsu C, Kuan K-Y, Chang C-F, Wang C-W, et al. Luteolin phosphate derivatives generated by cultivating *Bacillus subtilis* var. Natto BCRC 80517 with Luteolin. *J Agric Food Chem*. (2022) 70:8738–45. doi: 10.1021/acs.jafc.2c03524

35. Strober B, Ryan C, van de Kerkhof P, van der Walt J, Kimball AB, Barker J, et al. Recategorization of psoriasis severity: Delphi consensus from the international psoriasis council. *J Am Acad Dermatol.* (2020) 82:117–22. doi: 10.1016/j.jaad.2019.08.026
36. Korman NJ. Management of psoriasis as a systemic disease: what is the evidence? *Br J Dermatol.* (2019) 182:840–8. doi: 10.1111/bjd.18245
37. Hidalgo-Cantabrana C, Gómez J, Delgado S, Requena-López S, Queiro-Silva R, Margolles A, et al. Gut microbiota dysbiosis in a cohort of patients with psoriasis. *Br J Dermatol.* (2019) 181:1287–95. doi: 10.1111/bjd.17931
38. Pangilinan Mary Catherine G, Sermswan P, Asawanonda P. Use of anti-IL-17 monoclonal antibodies in HIV patients with Erythrodermic psoriasis. *Case Rep Dermatol.* (2020) 12:132–7. doi: 10.1159/000508781
39. Zhou F, Zhu Z, Gao J, Yang C, Wen L, Liu L, et al. RETRACTED: NFKB1 mediates Th1/Th17 activation in the pathogenesis of psoriasis. *Cell Immunol.* (2018) 331:16–21. doi: 10.1016/j.cellimm.2018.04.016
40. Zhao JDT, Wang Y, Wang Y, Liu X, Liang D, Li P. Paeoniflorin inhibits imiquimod-induced psoriasis in mice by regulating Th17 cell response and cytokine secretion. *Eur J Pharmacol.* (2016) 772:131–43. doi: 10.1016/j.ejphar.2015.12.040
41. Yang B-Y, Cheng Y-G, Liu Y, Liu Y, Tan J-Y, Guan W, et al. Ameliorates Imiquimod-induced psoriasis-like dermatitis and inhibits inflammatory cytokines production through TLR7/8–MyD88–NF- $\kappa$ B–NLRP3 Inflammasome pathway. *Molecules.* (2019) 24:2157. doi: 10.3390/molecules24112157
42. Murawska-CiaLowicz E, Jethon Z, Magdalan J, Januszewska L, Podhorska-OkoLów M, Zawadzki M, et al. Effects of melatonin on lipid peroxidation and antioxidative enzyme activities in the liver, kidneys and brain of rats administered with benzo(a)pyrene. *Exp Toxicol Pathol.* (2011) 63:97–103. doi: 10.1016/j.etp.2009.10.002
43. Yaling J, Wenyuan L, Shuang F. Research progress on structural modification and biological activity of luteolin [J]. *Chin. Herb. Med.* (2023) 54:6889–02. doi: 10.7501/j.issn.0253-2670.2023.20.032